

Phase-Sensitive T1 Inversion Recovery Imaging: A Time-Efficient Interleaved Technique for Improved Tissue Contrast in Neuroimaging

Ping Hou, Khader M. Hasan, Clark W. Sitton, Jerry S. Wolinsky, and Ponnada A. Narayana

BACKGROUND AND PURPOSE: High tissue contrast and short acquisition time are desirable when scanning patients. The purpose of this report is to describe the implementation of a new technique for generating high gray matter (GM) and white matter (WM) contrast in a short scan time, make a quantitative evaluation of the contrast efficiency, and explore its potential applications in neuroimaging.

METHOD: A fully interleaved T1-weighted inversion recovery (T1IR) sequence with phase-sensitive reconstruction (PS-T1IR) is implemented. This sequence is compared with conventional T1-weighted spin-echo imaging (T1SE) and T1-weighted fluid-attenuated inversion recovery (T1FLAIR). The time efficiency and contrast enhancement have been quantitatively analyzed in normal volunteers. The performance of the sequence is evaluated in >30 patients with neurologic disorders. The sensitivity of PS-T1IR relative to T1SE in detecting gadolinium enhancements is also evaluated.

RESULTS: PS-T1IR is more time-efficient than T1SE and generates better GM-WM contrast. It results in the best contrast-to-noise ratio (CNR) efficiency (1.16) compared with T1FLAIR (0.73) and T1SE (0.23). For a typical clinical protocol, PS-T1IR takes only 1:30 minutes versus 2:40 minutes for T1SE imaging for the whole brain coverage. Although gadolinium enhancements are detected with comparable sensitivity on both PS-T1IR and T1SE sequences, in certain instances, the latter sequence appears to be more sensitive in demonstrating gadolinium enhancements within WM.

CONCLUSION: PS-T1IR has the highest CNR efficiency compared with T1FLAIR and T1SE. It is a very practical technique for neuroradiologic applications.

Inversion recovery (IR) sequences are commonly used to suppress the MR signal intensity from CSF (1–2) or fat; the so-called fluid-attenuated inversion recovery (FLAIR) and short tau inversion recovery (STIR) sequences (3), respectively. In addition to suppressing specified tissues, IR pulse sequences can generate T1-weighted images with an intermediate inversion time (TI) of 600–1,200 milliseconds. Several studies have also demonstrated that IR provides superior contrast and greater sensitivity in detecting gadolinium (Gd) contrast enhancement than conven-

tional spin-echo (SE) sequences (4–8). STIR generates high-contrast T1-, T2-, and proton density-weighted images by nulling the fat signal. Like most IR sequences, however, STIR requires long acquisition time, even when combined with the fast spin-echo (FSE) readout. A time-efficient interleaved technique was proposed by Listerud et al (9) for acquiring T2-weighted FLAIR (T2FLAIR) images. In their technique, section excitation and acquisition were both interleaved during the TI and TR periods. This interleaved technique can be adapted for acquiring T1-weighted image. With this truly section and time interleaved technique, the contrast between white matter (WM) and gray matter (GM) is improved by suppressing CSF. Because the T1-weighted FLAIR (T1FLAIR) images are generated by magnitude reconstruction, gain in the image contrast, however, remains limited. Moreover, the images appear blurred compared with conventional T1-weighted SE (T1SE) images. Therefore, despite its speed and robustness, T1FLAIR did not gain wide acceptance in the radiologic community, and T1SE continues to be

Received December 17, 2004; accepted after revision February 1, 2005.

From the Departments of Diagnostic and Interventional Imaging (P.H., K.M.H., C.W.S., P.A.N.) and Neurology (J.S.W.), University of Texas Medical School at Houston, Houston, TX.

Address correspondence to Ping Hou, PhD, Department of Diagnostic and Interventional Imaging, University of Texas Medical School at Houston, 6431 Fannin Street, MSB 2.100, Houston, TX 77030.

© American Society of Neuroradiology

the sequence of choice for generating T1-weighted images.

Central to all the inversion recovery sequences is the application of an inversion radio-frequency (RF) pulse that flips the longitudinal magnetization from the +z to the -z direction. The magnetization can, therefore, be positive or negative, depending on the TI and tissue T1 values and the time at which the readout sequence is applied. By preserving the sign of the MR signal intensity, the image contrast can be enhanced by selecting appropriate TI value (10, 11). The benefits of the phase-sensitive reconstruction in IR are well known (10–18). Its application, however, has been limited by the artifacts from phase errors and long scan times. The sources of phase errors include non-centering of the echo in the readout window because of errors in the pulse sequence timing and phase-encoding steps, phase shifts from hardware such as bandwidth filters, variation in the patient loading, and coil sensitivity. Different phase-correction strategies, including acquisition of a reference image (16, 17) and estimation of phase from local statistics (10, 11, 15), have been investigated. In this article, we apply the phase-sensitive reconstruction to an interleaved T1-weighted IR pulse sequence (PS-T1IR) for generating images with high tissue contrast in a short scan time and demonstrate its application in neuroimaging.

Methods

Theory

The signal intensity amplitude in an IR sequence (19) can be written as

$$S_{IR}(TI, TE, TR) = \rho(1 - 2e^{-TI/T_1} + 2e^{-(TR-TE/2)/T_1} - e^{-TR/T_1})e^{-TE/T_2}$$

where ρ is the water proton spin density and the other symbols have their usual meaning. The T1 weighting is determined by the expression in the parenthesis and we refer to this as the T1-weighted factor. It can be seen from the above expression that the T1 contrast in an IR sequence is different from that of the SE sequence. The T1-weighted factor is a function of both TR and TI, which are user-selectable and is negative for a short TI and positive for long TI. The advantage of the phase-sensitive reconstructed IR is that the range of the T1-weighted factor is from -1 to 1 instead of 0 to 1 in a T1SE sequence. This increased dynamic range provides greater T1 contrast for different tissues. Because, in practice, TR is not infinite, the actual dynamic range is within $-(1 - \exp[-TR/T_1])$ to $(1 - \exp[-TR/T_1])$. The traditional magnitude reconstruction in the IR sequence automatically restricts the range of the T1-weighted factor from 0 to $(1 - \exp[-TR/T_1])$, and has the potential disadvantage of compromising the contrast between tissues, depending on the value of TI, as demonstrated in Figure 1. It can be observed from Figure 1 that, if the inversion time is set between 400–500 milliseconds, the WM and GM have opposite magnetizations; their contrast in the magnitude-reconstructed images appears minimal. In addition to the potential loss of contrast, magnitude IR images also suffer from the dark line artifact that appears at the tissue borders where the positive and negative signals cancel. The phase-sensitive reconstruction not only suppresses this dark line artifact, but also provides improved GM-WM contrast and hypointense CSF signal intensity, because it has a large negative magnetization.

The fully interleaved T1IR sequence is shown in Figure 2. If

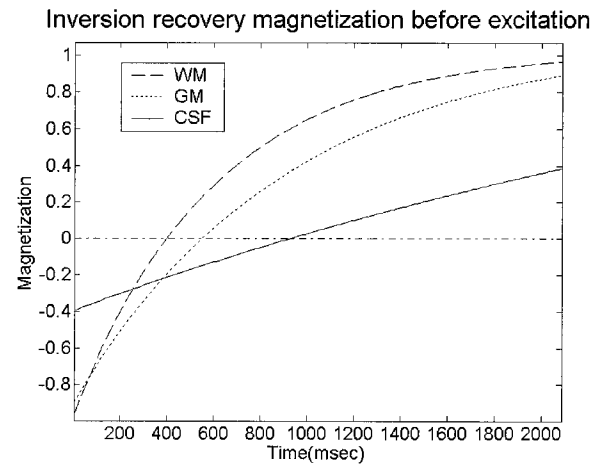


FIG 1. Behavior of longitudinal magnetization as a function of inversion time before the application of the read-out sequence. The parameters used in these simulations are TR, 2250 milliseconds; T1WM, 600 milliseconds; T1GM, 920 milliseconds; and T1CSF, 4200 milliseconds.

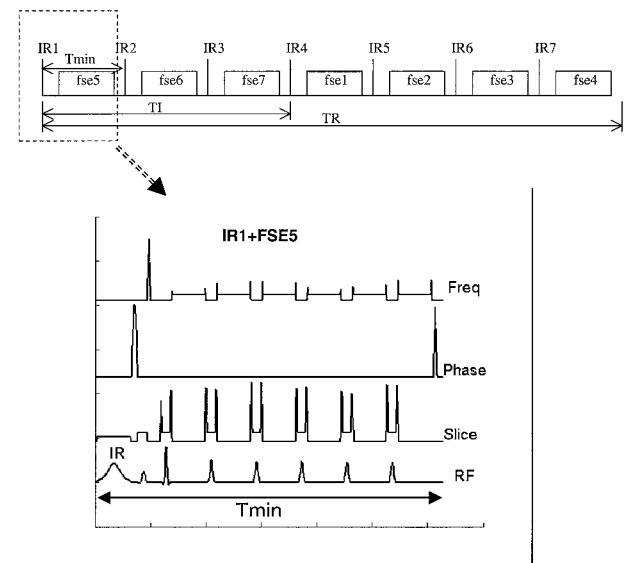


FIG 2. Timing diagram of the T1IR sequence. In this diagram, the number of sections packed in one TI is 3, and the maximum number of sections covered in one TR is 7. The upper part shows the interleaved scheme, and the lower part shows how the IR and FSE integrate tightly in timing. T_{min} is the time of IR, crusher gradient (in the phase encoding direction) and the FSE acquisition time. If the number of sections packed in the TI is less than the maximum sections allowed, there is a delay time added between crusher gradient and the FSE, and T_{min} stays the same.

the minimum sequence play out time is defined as T_{min} , which includes the inversion RF pulse, crusher gradients, and FSE data acquisition time, the number of sections covered during inversion time (TI) is TI/T_{min} , and the total number of sections in one repetition time (TR) is TR/T_{min} . The number of sections covered in TI and TR is truncated to an integer and is further reduced because of the hardware idle time requirements (gradient recovery, delay between the transmitter inactivation and receiver activation, and so forth) and RF safety limitations. Each IR pulse is followed by a readout sequence (FSE, in this case) with a different excitation frequency for specific section location. There is no dead time left in the pulse sequence. This is an optimal approach for time and section interleaving.

Subject and Protocols

Five healthy volunteers were scanned with T1SE, T1FLAIR, and PS-T1IR sequences. Both T1SE and PS-T1IR images were acquired on 30 patients with neurologic diseases. Twenty of these patients were administered Gd-diethylene triamine pentaacetic acid as a part of the diagnostic procedure. All volunteers signed the consent form before scanning, in accordance with our institutional regulations.

All scans were performed on a GE 1.5T Signa system (GE Medical Systems, Waukesha, WI) equipped with a gradient system capable of generating maximum gradient amplitude of 40 mT/m per channel with a slew rate of 150 mT/m/msec. A standard quadrature head coil was used for RF transmission and reception. This sequence is based on the GE sequence, T1FLAIR. An adiabatic inversion pulse was used, because it is less sensitive to B1 field inhomogeneity and generates a more uniform section profile. Tailored RF pulses were used for all FSE data acquisition to reduce the echo-bounce artifacts (20). Conventional T1SE images, T1FLAIR images, and PS-T1IR images were acquired to compare the image contrast and scan times. In the PS-T1IR sequence used in the current studies, the echo train length was 6 with an echo spacing of 11.4 ms. The other parameters were $T_{\min} = 88.5$ ms and $TR = 2250$ ms. Concatenation was not used. Acquisition and image matrices were the same for all the scans (256×192 constructed to 256×256 , FOV of 24 cm). For normal volunteers, the total number of sections was 42 with a thickness of 3 mm and no gap. For patients the total number of sections was 19–21, with a section thickness of 5 mm and a 2.5-mm gap, as determined by the radiologist. For all scans, the k-space raw data were saved automatically to reconstruct either real or magnitude images.

Unlike the magnitude imaging in which specific tissue is suppressed for improved contrast, the contrast enhancement in PS-T1IR images is not as sensitive to the choice of the inversion time. Although the T1 values for CSF, GM, and WM vary somewhat from patient to patient, the PS-T1IR images yielded consistent contrast in all patients with the same TI and TR values. In our application, varying TI between 400 milliseconds and 500 milliseconds had little effect on the contrast. Therefore, a TI of 430 milliseconds was selected purely for time efficiency to maximize the number of sections for a given TR and TI.

Data Analysis

To quantify the combined effect of CNR and the total imaging time (in analogy with a previously used SNR efficiency factor) (21), we define the contrast efficiency figure of merit between tissue 1 and tissue 2 as

$$\left(\eta_{12} = \frac{CNR_{12}}{\sqrt{\text{scantime}}} \right)$$

Here the CNR_{12} is defined as signal intensity difference between tissues one and 2 divided by the noise:

$$\left(CNR_{12} = \frac{|S_1 - S_2|}{\sigma} \right)$$

S_1 and S_2 are the signal intensities from tissues 1 and 2, respectively, and σ represents the noise.

The phase-sensitive reconstruction method that is built into the GE Signa scanner is based on the local phase statistics and a smooth background phase and a region-grow algorithm is used (11). In our studies, however, this produced unexpected intensity inversion from section to section. We have therefore incorporated an edge detection algorithm to automatically correct for these unexpected intensity inversions. These images were automatically exported back to the browser on the scanner with a real-time son-of-recon.

Results

Typical images of a normal volunteer at two different locations (lateral ventricular and cerebellar levels) acquired with T1SE, T1FLAIR, and PS-T1IR sequences are shown in Figure 3. The details about the acquisition parameters are given in the caption. The scan times for both T1FLAIR and PS-T1IR are comparable (2.38 and 2.33 minutes, respectively), whereas the scan time for the T1SE images was 3.28 minutes. These images clearly show the superior GM-WM contrast at both the locations on the PS-T1IR images (with the shortest scan time) compared with the T1FLAIR and T1SE images. Signal intensities from various WM structures (forceps minor, genu of the corpus callosum, internal capsule) and GM structures (head of caudate nucleus, putamen) were measured and the contrast efficiency was calculated for all five healthy volunteers by using the same imaging matrix and sections for PS-T1IR, T1FLAIR, and T1SE. The mean efficiency and the standard deviation are listed in Table 1. PS-T1IR showed the highest contrast efficiency (1.16). The Student's *t* test demonstrated significant contrast efficiency improvement from T1SE to PS-T1IR.

As an example, Figure 4 shows the PS-T1IR, T1SE, and T2-weighted FLAIR images of an 8-year-old girl with inflammatory demyelination. The FLAIR images (scan time 3 min 22 s) show the WM lesions quite clearly. But the GM-WM contrast on these images is not high. The T1SE image (scan time of 2 min 28 s) shows the poorest GM-WM contrast and lesion-to-background contrast. On the other hand, the PS-T1IR image (scan time of 1 min 25 s) shows excellent GM-WM contrast, WM to normal-appearing WM contrast. In addition, all the lesions seen on the FLAIR images can also be seen very clearly on the PS-T1IR images.

The T1SE sequence is most commonly used to detect the contrast enhancement in MR images. To evaluate the performance of the PS-T1IR sequence in detecting the contrast enhancements relative to the conventional T1SE sequence, postcontrast images were acquired with both sequences in 20 patients. Among the 20 patients who underwent Gd scans, seven enhancements were observed on both T1SE and PS-T1IR images. Visual comparison was performed for all the seven patients who had positive Gd response. Figure 5 shows, for example, the T2-weighted and pre- and postcontrast images of a patient with multiple cerebral abscesses. The PS-T1IR sequence showed Gd enhancement that was very similar to that seen on the conventional T1SE image. It can also be seen from this figure that both the T2 and T1SE images were degraded by motion, and the PS-T1IR images were relatively artifact-free because the patient did not move during scan.

In the current study, we observed the enhancing regions to be irregular, sometimes with very thin margins, and patchy in nature. This made the placement of the region of interest for quantitation of the CNR extremely difficult. Therefore, the relative perfor-

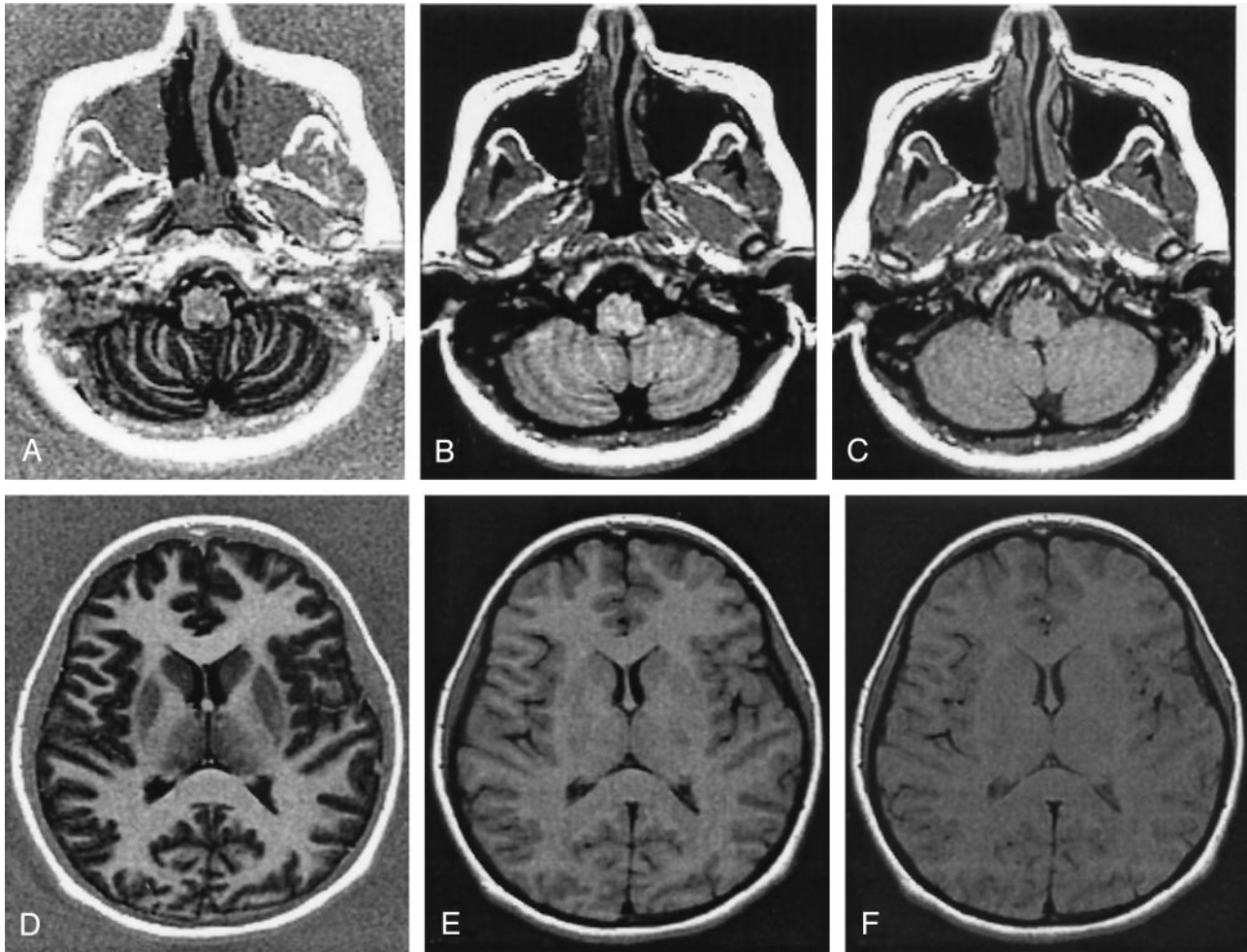


Fig 3. Axial images at two different locations of a normal volunteer acquired with three different sequences. The acquisition parameters for all the three sequences are: number of sections, 42; section thickness, 3.0 mm; gap, 0.0 mm; FOV, 24 cm \times 24 cm; acquisition matrix, 256 \times 192; receiver bandwidth, 15.63 kHz; NEX, 1.

A and D, PS-T1IR: TE, 11.5 milliseconds; TR, 2250 milliseconds; TI, 430 milliseconds; scan time = 2 min 33 s.

B and E, T1FLAIR: TE, 11.5 milliseconds; TR, 2250 milliseconds; TI, 977 milliseconds; scan time, 2 min 38 s.

C and F, T1SE: TE, 14 milliseconds; TR, 500 milliseconds; scan time, 3 min 28 s. The PS-T1IR demonstrates excellent GM-WM contrast and CSF is totally black, as predicted from theoretical simulation in Figure 1. The superior GM-WM contrast observed with the PS-T1IR sequence relative to the T1FLAIR and T1SE sequences can easily be appreciated on these figures.

Imaging contrast efficiency

Technique	PS-T1IR	T1FLAIR	T1SE
Scan time	2 min 33 s	2 min 38 s	3 min 28 s
η_{12}	1.159 \pm 0.086	0.729 \pm 0.169	0.232 \pm 0.115
<i>P</i>		0.0010	0.0000
η_{15}	0.908 \pm 0.174	0.398 \pm 0.152	0.120 \pm 0.118
<i>P</i>		0.0012	0.0000
η_{32}	1.198 \pm 0.092	0.729 \pm 0.160	0.156 \pm 0.151
<i>P</i>		0.0005	0.0000
η_{45}	0.816 \pm 0.147	0.407 \pm 0.276	0.097 \pm 0.099
<i>P</i>		0.0193	0.0000
η_{42}	1.067 \pm 0.111	0.738 \pm 0.164	0.209 \pm 0.125
<i>P</i>		0.0059	0.000

*The *P* value is from the Student *t*-test for unequal samples relative to PS-T1IR. The values are mean \pm sd. 1 indicates corpus callosum, forceps minor; 2, caudate nucleus, head; 3, corpus callosum, genu; 4, internal capsule, genu; and 5, putamen.

mances of these two sequences in terms of Gd enhancement were qualitatively evaluated by an experi-

enced neuroradiologist (C.W.S.). As assessed by the neuroradiologist, both T1SE and PS-T1IR sequences provided comparable contrast enhancement in six cases. In one case, however, the T1SE generated more accurate margin definition between WM and the enhanced stroke area than PS-T1IR, as shown in Figure 6.

Discussion

In these studies, we have demonstrated that the PS-T1IR sequence provides superior GM-WM contrast with clear lesion delineation at shorter scan time relative to both conventional SE and T1FLAIR sequences. The short acquisition time of the PS-T1IR sequence might help acquire images with reduced movement artifacts. Lee et al (8) applied the FSE-based T1IR sequence for imaging intracranial lesions and demonstrated increased contrast over the T1SE images. In applications of this type, PS-T1IR should

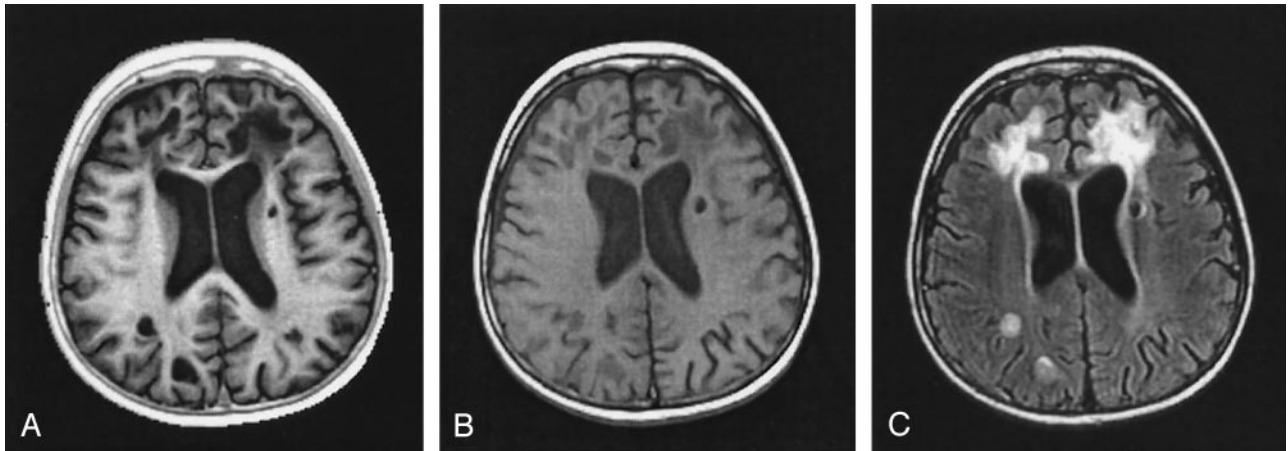


FIG 4. Images from an 8-year-old patient with inflammatory demyelination. PS-T1IR (A) displays much better GM-WM contrast than does regular T1SE (B) and better contrast between diseased areas of WM and normal-appearing ones (sparing of U-fibers is easily seen) with shorter scan time.

A, PS-T1IR: 256 × 192; 21 sections; FOV, 24 cm; TE, 11.5 milliseconds; TR, 2250 milliseconds; TI, 430 milliseconds; NEX, 1; receiver bandwidth, 15.63 kHz; section thickness, 5.0 mm; gap, 2.5 mm; scan time, 1:25 minutes.

B, T1SE: 256 × 192; 21 sections; FOV, 24 cm; TE, 14 milliseconds; TR, 500 milliseconds; NEX, 2; receiver bandwidth, 15.63 kHz; section thickness, 5.0 mm; gap, 2.5 mm; scan time, 2:28 minutes.

C, T2 FLAIR: FOV, 24 cm; 256 × 160; 21 sections; TE, 147 milliseconds; TR, 8800 milliseconds; TI, 2200 milliseconds; NEX, 1; receiver bandwidth, 15.63 kHz; section thickness, 5.0 mm; gap, 2.5 mm; scan time, 3:32 minutes. Note that the section location does not match perfectly, because of patient movement between scans.

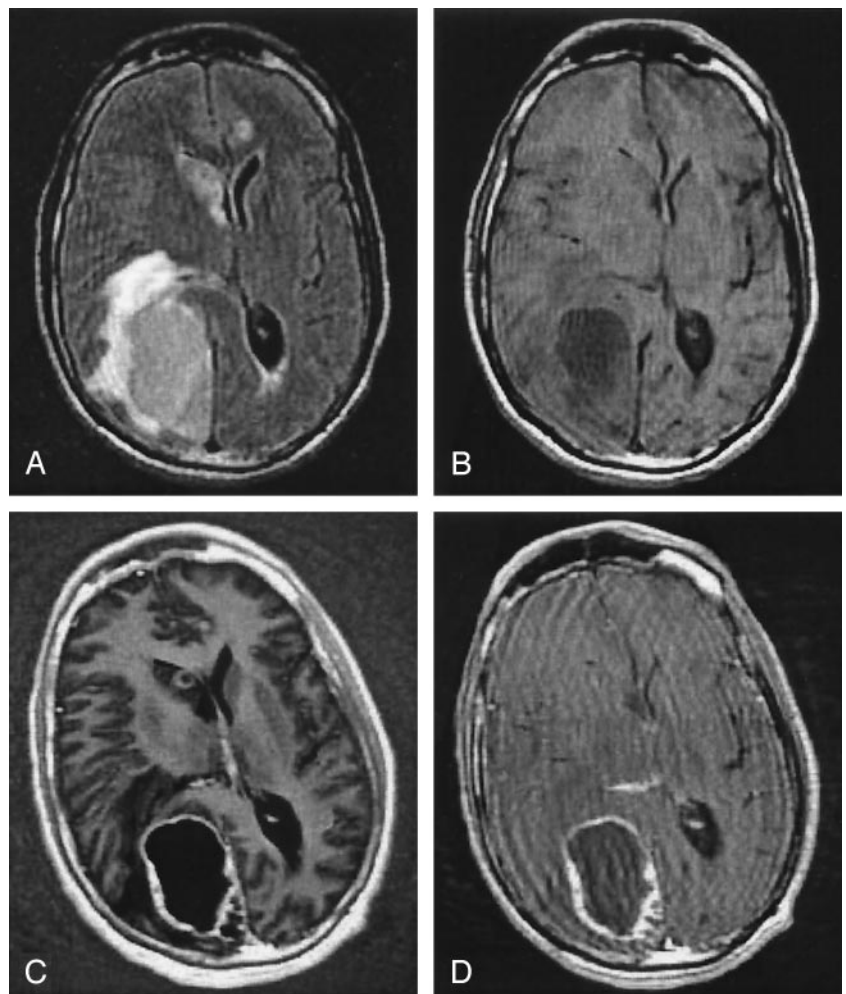
FIG 5. Axial images obtained in a patient with multiple cerebral abscesses.

A, Several well-circumscribed mass lesions with perilesional edema are seen on the T2 FLAIR images (FOV, 24 cm; 256 × 160; 20 sections; TE, 147 milliseconds; TR, 8800 milliseconds; TI, 2200 milliseconds; NEX, 1; receiver bandwidth, 15.63 kHz; section thickness, 5.0 mm; gap, 2.5 mm). The total scan time is 3:32 minutes.

B, Pre-Gd T1SE images. The acquisition parameters are acquisition matrix, 256 × 192; total number of sections, 20; section thickness, 5.0 mm; section gap, 2.5 mm; FOV, 24 cm × 18 cm; TE, 14 milliseconds; TR, 500 milliseconds; NEX, 2; receiver bandwidth, 15.63 kHz. The total scan time is 2:28 minutes.

C, Post-Gd PS-T1IR images. The acquisition parameters are acquisition matrix, 256 × 192; total number of sections, 19; section thickness, 5.0 mm; gap, 2.5 mm; FOV, 24 cm × 24 cm; TE, 11.5 milliseconds; TR, 2250 milliseconds; TI, 430 milliseconds; NEX, 1; receiver bandwidth, 15.63 kHz. The scan time is 1:25 minutes.

D, Post-Gd T1SE images acquired with identical parameters as the precontrast images in B. Notice the motion-induced degradation of the images acquired with the T2 FLAIR and T1SE sequences.



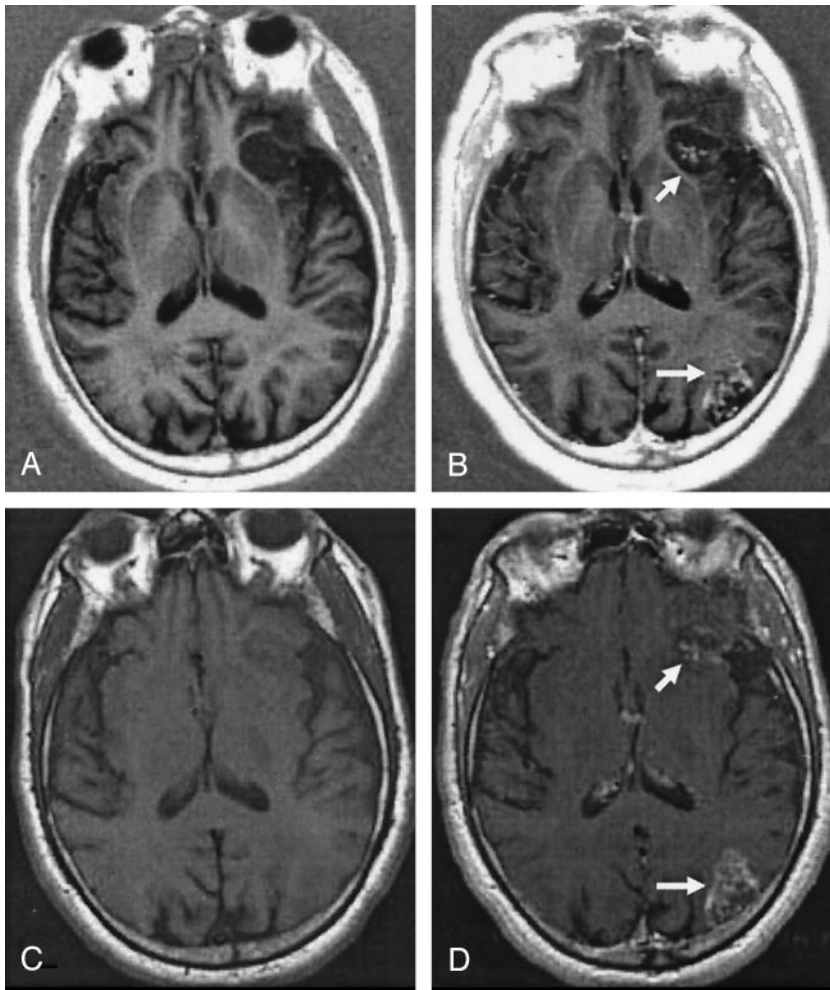


FIG 6. Pre- and postcontrast PS-T1IR (A, B) and T1SE images (C, D) from a 70-year-old male stroke patient. The slightly better margin definition of Gd-enhanced stroke (lower right corner of the image) on the T1SE image compared with the PS-T1IR image can be appreciated on these images; however, the lesion definition is superior on the PS-T1IR images. The top Gd-enhancement for PS-T1IR and T1SE (upper right corner of the image) are quite comparable because of the dark background. Note a slight mismatch between the pre- and postcontrast images because of the patient movement. The acquisition parameters for the (PS-T1IR, T1SE) images were TE, (12, 17) milliseconds; TR, (2184, 516) milliseconds; T1, (430, n/a) milliseconds; echo train length, (6, n/a); echo spacing, (11.4, n/a) milliseconds; NEX, (1, 2). The same values for FOV (24 cm \times 24 cm), section thickness (5 mm, skip 2.5 mm), and acquisition matrix (256 \times 192) were used for both the sequences.

provide even better tissue contrast with a shorter scan time. The enhanced contrast and clarity of the GM/WM interfaces seen on the PS-T1IR images should also be useful in the evaluation of cortical dysplasias and migrational abnormalities, particularly as it applies to the screening of epilepsy patients.

These studies also show that the PS-T1IR sequence detects Gd enhancement with a sensitivity that is comparable to the spin-echo T1SE sequence, at shorter acquisition times, in most of the cases. Shorter imaging times on post-Gd images would be advantageous for the evaluation of most infectious, inflammatory, and neoplastic processes, particularly because this requires acquiring images in multiple planes. Thus, the PS-T1IR sequence appears to be well suited for neuroimaging applications.

The PS-T1IR image reconstruction implicitly assumes a smooth background phase error. Therefore, currently only RF coils with homogenous RF profiles can be used for generating these images. Kellman et al (22, 23), on the basis of reference scan and B1 field sensitivity correction, recently demonstrated the application of phase-sensitive IR reconstruction for the detection of myocardial infarction with phased-array coils. In their application, the main purpose of using PSIR was to take advantage of the T1 insensitivity to contrast enhancement. Because the real part of the

signal intensity was used for final image reconstruction, phase-sensitive inversion recovery reconstruction not only generated excellent image contrast, but also provided better SNR (17, 18). Therefore, this sequence can potentially be combined with multielement coils for acquiring T1-weighted images at high fields at shorter acquisition times.

Finally, lesions appear hypointense on the PS-T1IR images, whereas they appear hyperintense on the FLAIR images. This difference in the appearance of lesions on images acquired with these two sequences along with excellent GM-WM contrast, combined with CSF suppression seen on PS-T1IR images, should greatly aid in the multispectral tissue segmentation for automatic tissue quantitation (24).

Conclusion

PS-T1IR is a very practical imaging sequence for clinical neuroradiologic applications. It provides excellent tissue contrast with short image acquisition time (1:30 minutes for whole brain with routine clinical parameters) compared with other IR and routine T1-weighted FSE sequences. PS-T1IR can detect Gd enhancement, but T1SE seems more sensitive to small T1 value decrease due to Gd injection. The

PS-T1IR images along with FLAIR images should be useful in automatic tissue segmentation.

Acknowledgments

Parts of these studies are supported by NIH grant EB02095 (to P.A.N.). The authors are grateful for the valuable discussions with Dr. Jingfei Ma at University of Texas—MD Anderson Cancer Center, Houston, Texas. Dr. Renjie He's help in image editing is greatly appreciated.

References

- Hajnal JV, Bryant DJ, Kasuboski L, et al. **Use of fluid attenuated inversion recovery (FLAIR) pulse sequences in MRI of brain.** *J Comput Assist Tomogr* 1992;16:841–844
- White SJ, Hajnal JV, Young IR, Bydder GM. **Use of fluid-attenuated inversion-recovery pulse sequences for imaging the spinal cord.** *Magn Reson Med* 1992;28:153–162
- Bydder G, Pennock J, Steiner R, et al. **The short TI inversion recovery sequence: an approach to MR imaging of the abdomen.** *Magn Reson Imaging* 1985;3:251–254
- Bydder G, Young IR. **MR imaging: clinical use of the inversion recovery sequence.** *J Comput Assist Tomogr* 1985;9:659–675
- Graif M, Bydder G, Steiner R, et al. **Contrast-enhanced MR imaging of malignant brain tumors.** *Am J Neuroradiol* 1985;6:855–862
- Melhem E, Jara H, Yucel E. **Multislice T1-weighted hybrid RARE in CNS imaging: assessment of magnetization transfer effects.** *J Magn Reson Imaging* 1996;6:903–908
- Rydberg J, Hammond C, Huston J, et al. **T1-weighted MR imaging of the brain using a fast inversion recovery pulse sequence.** *J Magn Reson Imaging* 1996;6:356–362
- Lee JK, Choi HY, Lee SW, et al. **Usefulness of T1-weighted image with fast inversion recovery technique in intracranial lesions: comparison with T1-weighted spin echo image.** *Clin Imaging* 2000;24:263–269
- Listerud J, Mitchell J, Bagley L, Grossman R. **Inversion recovery image reconstruction with multiseed region-growing spin reversal.** *Magn Reson Med* 1996;6:775–782
- Xiang QS. **Inversion recov. image reconstruct. with multiseed region-growing spin reversal.** *J Magn Reson Imaging* 1996;00:775–782
- Ma J. **Phase-sensitive inversion recovery method of MR imaging.** US patent. September 1998;6192263
- Young IR, Bailes DR, Bydder GM. **Apparent changes of appearance of inversion-recovery images.** *Magn Reson Med* 1985;2:81–85
- Gowland PA, Leach MO. **A simple method for the restoration of signal polarity in multi-image inversion recovery sequences for measuring T1.** *Magn Reson Med* 1991;18:224–231
- Ahn CB, Cho ZH. **A new phase correction method in NMR imaging based on autocorrelation and histogram analysis.** *IEEE Trans Med Imaging* 1987;6:32–36
- Borrello JA, Chenevert TL, Aisen AM. **Regional phase correction of inversion-recovery MR images.** *Magn Reson Med* 1990;14:56–67
- Park HW, Cho MH, Cho ZH. **Real-value representation in inversion-recovery NMR imaging by use of a phase-correction method.** *Magn Reson Med* 1986;3:15–23
- Noll DC, Nishimura DG, Macovski A. **Homodyne detection in magnetic-resonance-imaging.** *IEEE Trans Med Imaging* 1991;10:154–163
- Bernstein MA, Thomasson DM, Perman WH. **Improved detectability in low signal-to-noise ratio magnetic resonance images by means of a phase-corrected real reconstruction.** *Med Phys* 1989;16:813–817
- Hendrick RE, Raff U. **Image contrast and noise.** In: Stark DD, Bradley Jr WG, eds. *Magnetic resonance imaging.* Vol 1. 2nd ed. St. Louis: Mosby; 1992:109–144
- Le Roux P, Hinks RS. **Stabilization of echo amplitudes in FSE sequences.** *Magn Reson Med* 1993;30:183–191
- Parker DL, Gullberg GT. **Signal-to-noise efficiency in magnetic resonance imaging.** *Med Phys* 1990;17:250–257
- Kellman P, Arai AE, McVeigh ER, Aletras AH. **Phase sensitive inversion recovery for detecting myocardial infarction using gadolinium delayed hyperenhancement.** *Magn Reson Med* 2002;47:372–383
- Kellman P, Dyke CK, Aletras AH, et al. **Artifact suppression in imaging of myocardial infarction using B1-weighted phased-array combined phase-sensitive inversion recovery.** *Magn Reson Med* 2004;51:408–412
- Sajja BR, Datta S, He R, Narayana PA. **A unified approach for MS lesion segmentation on MR images.** *Proceedings of IEEE Engineering in Medicine and Biology Society (EMBS)* 2004;1778–1781